Photolysis of ferric ions in the presence of sulfate or chloride ions: implications for the photo-Fenton process†

Amilcar Machulek Jr.,*[a] José Ermírio F. Moraes,[b] Laura T. Okano,*[c] Cristina A. Silvério[c] and Frank H. Quina[d]

Received 12th January 2009, Accepted 11th May 2009
First published as an Advance Article on the web 26th May 2009
DOI: 10.1039/b900553f

The photo-Fenton process (Fe^{2+}/Fe^{3+}, H_2O_2, UV light) is one of the most efficient and advanced oxidation processes for the mineralization of the organic pollutants of industrial effluents and wastewater. The overall rate of the photo-Fenton process is controlled by the rate of the photolytic step that converts Fe^{3+} back to Fe^{2+}. In this paper, the effect of sulfate or chloride ions on the net yield of Fe^{2+} during the photolysis of Fe^{3+} has been investigated in aqueous solution at pH 3.0 and 1.0 in the absence of hydrogen peroxide. A kinetic model based on the principal reactions that occur in the system fits the data for formation of Fe^{2+} satisfactorily. Both experimental data and model prediction show that the availability of Fe^{2+} produced by photolysis of Fe^{3+} is inhibited much more in the presence of sulfate ion than in the presence of chloride ion as a function of the irradiation time at pH 3.0.

1. Introduction

Advanced oxidation processes (AOPs) have been widely studied for the oxidation of several types of industrial wastewater.[1,2] The production of powerful oxidizing agents, such as the hydroxyl radical, is the main objective of AOPs. The hydroxyl radical can react with organic compounds by hydrogen abstraction, addition to unsaturated bonds and aromatic rings, or electron transfer.[1,2] One of the most efficient AOPs is the photo-Fenton reaction (Fe^{2+}/Fe^{3+}, H_2O_2, UV light), which very successfully oxidizes a wide range of compounds such as arsenic(III) ions,[3] azo-dye compounds[4] and insecticides,[5] among others.[6–8]

In the thermal Fenton reaction, the hydroxyl radical is generated by the oxidation of Fe^{2+} to Fe^{3+} by hydrogen peroxide (eqn (1)).

$$Fe^{2+} + H_2O_2 \rightarrow Fe(III) + HO^{\bullet} + OH^{-} \quad (1)$$

When all of the Fe^{2+} has been converted to Fe^{3+}, the rate of the Fenton reaction slows down substantially due to the inefficient H_2O_2-mediated reduction of Fe^{3+} back to Fe^{2+}. However, upon irradiation of the Fenton reaction system by UV light, the reaction is accelerated due to the photolytic conversion of Fe^{3+} back to Fe^{2+}. In the photo-assisted Fenton reaction, the principal light-absorbing Fe^{3+} species present at pH 2.5–3.5 is $Fe(H_2O)_5(OH)^{2+}$, written for convenience as $Fe(OH)^{2+}$, formed by deprotonation of hexaquo Fe(III). Upon photolysis, $Fe(OH)^{2+}$ produces Fe^{2+} and a hydroxyl radical as products with a quantum yield of *ca.* 0.2 at 347 nm (eqn (2)).[9,10]

$$Fe(OH)^{2+} + h\nu \rightarrow Fe^{2+} + HO^{\bullet} \quad (2)$$

The oxidizing species present in the Fenton reaction responsible for the degradation processes are both the hydroxyl radical,[1,8,11] and the ferryl (denoted as FeO^{2+}) or Fe(IV) species.[11–13]

The control of the solution pH can substantially affect the overall yield of the photo-Fenton reaction. Typically, the initial pH of a photo-Fenton reaction is adjusted to *ca.* pH 3.0. However, as the degradation of the organic material proceeds, the pH of the reaction mixture falls rather rapidly to about pH 2 due to the formation of organic acids such as oxalic acid. Under these conditions, the photo-Fenton reaction is strongly inhibited by the presence of added chloride ions (≥ 0.03 mol L^{-1} of Cl^{-}).[14,15] In a previous study,[16,17] we employed nanosecond laser flash photolysis to demonstrate that the inhibition of the photochemical step of the photo-Fenton reaction by chloride ions results from a combination of two factors, *viz.*, competitive complexation of Fe^{3+} by Cl^{-} and the pH-dependent scavenging of the hydroxyl radical by the chloride ion. Both events produce chlorine atoms as the product, which react with chloride ions to form the much less reactive species $Cl_2^{\bullet-}$.[10,16–18] In a previous work,[16,17] we developed a kinetic model that reproduced the kinetics of formation and decay of $Cl_2^{\bullet-}$ on the nanosecond to microsecond time scale as a function of concentration of Fe^{3+}, chloride ion and pH. However, the photo-Fenton reaction is typically performed under continuous irradiation and in the presence of H_2O_2 when employed for wastewater treatment. The wastewater may contain inorganic anions such as chloride or sulfate ions or they can be added as part of the reagents ($FeSO_4$, H_2SO_4, HCl, $FeCl_3$) used for the mineralization process.[18]

In the present paper, we extend our earlier kinetic model by including several new reactions in order to describe the effect of added chloride and sulfate ions on net yield of Fe^{2+} in the absence of H_2O_2 in the photochemical step of the photo-Fenton reaction on a long-time scale. We have chosen the experimental condition of total absence of added H_2O_2 since the presence of hydrogen peroxide would rapidly convert Fe^{2+} to Fe^{3+} and thereby make

[a]*Faculdade de Ciências Exatas e Tecnologia, Universidade Federal da Grande Dourados, Mato Grosso do Sul, 79804-970, MS, Brazil. E-mail: machulekjr@gmail.com*
[b]*Universidade Federal de São Paulo, Diadema, 09972-270, SP, Brazil*
[c]*Departamento de Química, Faculdade de Filosofia, Ciências e Letras de Ribeirão Preto, Universidade de São Paulo, Av. dos Bandeirantes 3900, Ribeirão Preto, 14040-901, SP, Brazil. E-mail: lauokano@usp.br*
[d]*Instituto de Química, Universidade de São Paulo, CP 26077, São Paulo, 05513-970, SP, Brazil*
† This article was published as part of the themed issue in honour of Esther Oliveros.

it impossible to evaluate the interference caused by chloride or sulfate ions on the net yield of Fe^{2+}.

2. Experimental

2.1. Materials

Sodium perchlorate (98%, sulfate ≤ 20 ppm and lead ≤ 5 ppm), anhydrous oxalic acid (p.a.), 1,10-phenanthroline monohydrate (99+%), iron(III) sulfate pentahydrate (97%), and iron(II) sulfate heptahydrate (p.a.) were purchased from Acros Organics. Sodium acetate trihydrate, sodium chloride (p.a., 0.003% sulfate and 2 ppm lead) were obtained from J. T. Baker. Ferric perchlorate hydrate (low chloride) and sulfuric acid (p.a.) were purchased from Aldrich and Mallinckrodt, respectively. All reagents were used as received.

2.2. Irradiations

All experiments were performed in a darkroom, using a merry-go-round reactor[19] equipped with four 8 W black light lamps (Sylvania Model BL350). According to the manufacturer's specifications, the emission of the phosphor of these UV-fluorescent lamps ranges from 300–400 nm with a maximum at 356 nm. Aliquots (3.0 mL) of aqueous solutions of ferric perchlorate or ferric sulfate in the absence or presence of NaCl (as source of chloride ion) were irradiated in 13 × 100 mm Pyrex culture tubes at a constant ionic strength of 1.0, pH 3.0 and 1.0. The concentrations of Fe^{3+}, sulfate, and chloride ions were 1.0–1.2 × 10^{-3}, 1.8 × 10^{-3} and 0.75 mol L^{-1}, respectively. Perchloric acid and sodium perchlorate were used to adjust the pH and the ionic strength, respectively. At appropriate time intervals, the test tubes were withdrawn and the concentration of Fe^{2+} present quantified *via* the formation of the Fe^{2+}-*o*-phenanthroline complex under the same conditions employed for ferrioxalate actinometry.[19] Incident photon intensities, determined by standard potassium ferrioxalate actinometry,[19] were 3.14 × 10^{-10} Ein s^{-1} per culture tube. All absorption spectroscopic measurements were performed with a Hitachi U-3000 UV-vis spectrophotometer. The irradiation experiments were performed in triplicate.

The rates of Fe^{2+} formation (in mol L^{-1} s^{-1}) were calculated according to eqn (3):[20]

$$\frac{\mathrm{d}[\mathrm{Fe}^{2+}]}{\mathrm{d}t} = \frac{I \quad F_{\mathrm{abs}} \quad \Phi}{V} \tag{3}$$

where I is the incident photon intensity (Ein s^{-1}); V the total volume of irradiated solution; Φ the global quantum yields for formation of Fe^{2+}. The fraction of the incident irradiation effectively absorbed by the solution, F_{abs}, was estimated from the relationship:

$$F_{\mathrm{abs}} = \int f_{\mathrm{abs}}(\lambda)\left[\frac{I(\lambda)}{\int I(\lambda)\mathrm{d}\lambda}\right]\mathrm{d}\lambda \tag{4}$$

which represents the integral of the relative intensity of the incident excitation light, $I(\lambda)$, defined such that $\int I(\lambda)\mathrm{d}\lambda = 1$, multiplied by the fraction of the incident light absorbed by the solution at each wavelength, f_{abs}, between 300 and 400 nm:

$$f_{\mathrm{abs}} = 1 - 10^{-A(\lambda)} \tag{5}$$

3. Results and discussion

Four experimental conditions (A–D) were chosen to evaluate the net production of Fe^{2+} from ferric ions under continuous irradiation at an ionic strength of 1.0, adjusted with sodium perchlorate. At pH 3.0, the photolysis was carried out with 1.0 mmol L^{-1} ferric ion: (A) without any added salt; (B) with added 0.75 mol L^{-1} chloride; and (C) with sulfate ions. In this last condition, we employed 0.6 mmol L^{-1} ferric sulfate, containing a total of 1.2 mmol L^{-1} Fe^{3+} and 1.8 mmol L^{-1} sulfate ions, without added chloride ions. At pH 1.0, (D) the photolysis of 1.0 mmol L^{-1} ferric perchlorate in the presence of 0.75 mol L^{-1} chloride ions, without sulfate ions, was investigated. Formation of the ferrous ion was monitored by UV-vis spectroscopy after complexation with *o*-phenanthroline.

At pH 3.0, the photolysis of an aqueous solution of ferric ion in the absence of any added salt (case A) is dominated by the photoreactivity of $Fe(OH)^{2+}$ (eqn (2)). The addition of chloride ions (case B) results in formation of $Fe(Cl)^{2+}$, which has a higher absorptivity and a higher quantum yield of photolysis of 0.47 at 347 nm.[10] (eqn (6))

$$\mathrm{Fe(Cl)}^{2+} + h\nu \rightarrow \mathrm{Fe}^{2+} + \mathrm{Cl}^{\bullet} \tag{6}$$

The presence of sulfate ions (case C) leads to formation of $FeSO_4^+$, which has a very low photolysis quantum yield of 0.0016 at 350 nm.[21] (eqn (7))

$$\mathrm{FeSO_4}^{+} + h\nu \rightarrow \mathrm{Fe}^{2+} + \mathrm{SO_4}^{-} \tag{7}$$

At pH 1, (case D) $Fe(Cl)^{2+}$ is the predominant species and absorbs most of the incident radiation.

Fig. 1 shows the experimental data for the formation of Fe(II) upon photolysis of the ferric ion solutions under these four conditions, together with the best fit curves calculated from our kinetic modelling (*vide infra*).

In the absence of chloride ions and other ligands, the major ionic species present in aqueous solutions of ferric ion are Fe^{3+}, $Fe(OH)^{2+}$, $Fe(OH)_2^+$ and/or $[Fe_2(OH)_2]^{4+}$, depending on the pH.[22] At pH less than 4.0, $Fe(OH)^{2+}$ is the predominant species present. Irradiation of $Fe(OH)^{2+}$ generates Fe^{2+} ions and hydroxyl radicals, with a quantum yield (ϕ) of 0.21 at 347 nm.[10] (eqn (2)).

However, $Fe_2(OH)_2^{4+}$ has the highest molar absorptivity in the UV (ε_{356} = 5000 mol^{-1} L cm^{-1}, as compared to ε_{356} = 800 and 550 mol^{-1} L cm^{-1} for $Fe(OH)^{2+}$ and $Fe(OH)_2^+$, respectively, and only ε_{356} = 10 mol^{-1} L cm^{-1} for Fe^{3+}).[9,22,23] Despite the high molar absorptivity of $[Fe_2(OH)_2]^{4+}$, the $\phi_{350\,nm}$ of hydroxyl radical production upon irradiation of this species is negligible (0.007).[24]

In modelling the kinetics of formation of Fe(II) *via* the photolysis of Fe(III) at pH 3.0 in the absence of chloride or sulfate, the reactions of Table 1 were employed. The speciation of Fe(II) was calculated using reactions 8–10 of this Table. The photolysis of $FeOH^{2+}$ and $Fe(OH)_2^+$ produces the hydroxyl radical (eqn (2)) and, together with reactions 17, and 18 of Table 1, produces ferrous ions. Reactions 11–14 of Table 1 summarize the reactions of the hydroxyl and peroxyl radicals and reactions 15 and 16 (Table 1) consume Fe^{2+} ions to regenerate ferric species. As shown in Fig. 1A, the resulting fit of the model to the data is quite satisfactory.

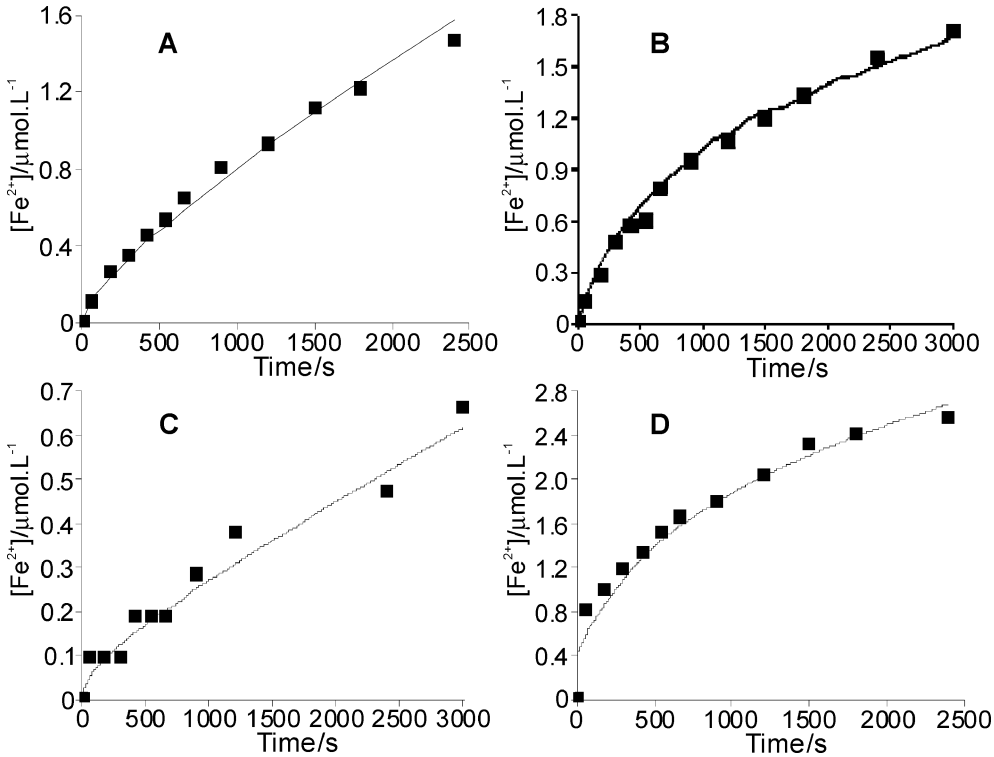

Fig. 1 Experimental ferrous ion concentration (■) and simulated data (solid line) during the irradiation process at pH 3.0 in: (A) the absence of chloride or sulfate ions; (B) $[Cl^-] = 0.75$ mol L^{-1}, absence of sulfate ions; (C) $[SO_4^{2-}] = 1.8$ mmol L^{-1}, absence of chloride ions, and (D) at pH 1.0 with $[Cl^-] = 0.75$ mol L^{-1}, absence of sulfate ions.

Table 1 Ground state reactions employed in the kinetic model for the photolysis of Fe(III) ions[a] in aqueous solution in the absence of SO_4^{2-} and Cl^- ions ($I = 1$)

No.	Reaction	k/s^{-1} or mol^{-1} L s^{-1}	Ref.
Speciation equilibria ($I = 1$)			
8	$Fe^{3+} + H_2O \rightleftarrows FeOH^{2+} + H^+$	$k_8 = 1.91 \times 10^7$[b], $k_{-8} = 1 \times 10^{10}$ $k_8 = 2.34 \times 10^7$	31
9	$Fe^{3+} + 2H_2O \rightleftarrows Fe(OH)_2^+ + 2H^+$	$k_9 = 3.39 \times 10^3$[b], $k_{-9} = 1 \times 10^{10}$ $k_9 = 4.68 \times 10^3$	31
10	$2Fe^{3+} + 2H_2O \rightleftarrows [Fe_2(OH)_2]^{4+} + 2H^+$	$k_{10} = 1.12 \times 10^7$, $k_{-10} = 1 \times 10^{10}$	31
Reactions of reactive oxygen radicals			
11	$HO^{\bullet} + HO^{\bullet} \rightarrow H_2O_2$	$k_{11} = 6.0 \times 10^9$	16
12	$HO^{\bullet} + H_2O_2 \rightarrow H_2O + HO_2^{\bullet}$	$k_{12} = 2.7 \times 10^7$	32
13	$HO_2^{\bullet} + HO_2^{\bullet} \rightarrow H_2O_2 + O_2$	$k_{13} = 8.3 \times 10^5$	31
14	$HO_2^{\bullet} + H_2O_2 \rightarrow HO^{\bullet} + O_2 + H_2O$	$k_{14} = 0.5$	31
Reactions of iron species			
15	$Fe^{2+} + HO^{\bullet} \rightarrow$ Fe(III)[a] $+ OH^-$	$k_{15} = 4.3 \times 10^8$[b] $k_{15} = 2.7 \times 10^8$, $k_{15} = 3.2 \times 10^8$	31,32
16	$Fe^{2+} + H_2O_2 \rightarrow$ Fe(III) $+ HO^{\bullet} + OH^-$	$k_{16} = 63$	32
17	Fe(III) $+ HO_2^{\bullet} \rightarrow Fe^{2+} + O_2 + H^+$	$k_{17} = 1 \times 10^6$	33
18	Fe(III) $+ H_2O_2 \rightarrow Fe^{2+} + HO_2^{\bullet} + H^+$	$k_{18} = 0.01$	32

[a] Fe(III) represents all Fe(III) species (Fe^{3+}, $FeOH^{2+}$ and $Fe(OH)_2^+$) in the absence of chloride or sulfate ion. [b] Unless otherwise indicated, the rate constant values were the ones that best fit our experimental data.

The addition of chloride ions to an aqueous solution of ferric ion results in competitive formation of $Fe(Cl)^{2+}$ and $Fe(Cl)_2^+$. Although $Fe(OH)^{2+}$ is still the predominant species at pH 3.0, $Fe(Cl)^{2+}$ and $Fe(Cl)_2^+$ have higher molar absorptivities (ε_{356} = 1600 mol^{-1} L cm^{-1} and 2740 mol^{-1} L cm^{-1}, respectively)[25] than $Fe(OH)^{2+}$ and $Fe(OH)_2^+$ in the ultraviolet and photodecompose with higher quantum yields. At pH 1.0, $Fe(Cl)^{2+}$ is predominant and responsible for the absorption of most of the

Table 2 Additional reactions employed in the kinetic model for the photolysis of Fe(III) ions[a] in aqueous solution in the presence of chloride and sulfate ions ($I = 1$)

No.	Reaction	k/s^{-1} or mol^{-1} L s^{-1}	Ref.
Speciation equilibria ($I = 1$)			
19	$Fe^{3+} + Cl^- \rightleftarrows FeCl^{2+}$	$k_{19} = 4.79 \times 10^{10}$[b], $k_{-19} = 1 \times 10^{10}$ $k_{19} = 6.61 \times 10^{10}$	31
20	$Fe^{3+} + 2\ Cl^- \rightleftarrows FeCl_2^+$	$k_{20} = 6.31 \times 10^{10}$[b], $k_{-20} = 1 \times 10^{10}$ $k_{20} = 1.05 \times 10^{11}$	31
Reactions of iron species			
21	$Fe^{2+} + Cl^{\bullet} \rightarrow$ Fe(III)[a] $+ Cl^-$	$k_{21} = 5.9 \times 10^9$	31
22	$Fe^{2+} + Cl_2^{\bullet -} \rightarrow$ Fe(III) $+ 2Cl^-$	$k_{22} = 5 \times 10^6$	31
Reactions of reactive chlorine species			
23	$Cl^{\bullet} + Cl^- \rightleftarrows Cl_2^{\bullet -}$	$k_{23} = 7.8 \times 10^9$, $k_{-23} = 5.7 \times 10^4$	31
24	$Cl^{\bullet} + H_2O_2 \rightarrow HO_2^{\bullet} + Cl^- + H^+$	$k_{24} = 1 \times 10^9$	31
25	$Cl_2^{\bullet -} + Cl_2^{\bullet -} \rightarrow 2Cl^- + Cl_2$	$k_{25} = 2.8 \times 10^9$	15
26	$Cl_2^{\bullet -} + H_2O_2 \rightarrow HO_2^{\bullet} + 2Cl^- + H^+$	$k_{26} = 1.4 \times 10^5$	31
27	$Cl_2^{\bullet -} + HO_2^{\bullet} \rightarrow 2Cl^- + H^+ + O_2$	$k_{27} = 3.1 \times 10^9$	31
28	$Cl^- + HO^{\bullet} \rightleftarrows HOCl^{\bullet -}$	$k_{28} = 4.2 \times 10^9$, $k_{-28} = 6.1 \times 10^9$[b] $k_{-28} = 6.0 \times 10^9$	31
29	$HOCl^{\bullet -} + H^+ \rightleftarrows H_2O + Cl^{\bullet}$	$k_{29} = 2.4 \times 10^{10}$, $k_{-29} = 1.8 \times 10^5$	31
30	$Cl_2^{\bullet -} + Cl^{\bullet} \rightarrow Cl^- + Cl_2$	$k_{30} = 1.4 \times 10^9$[b] $k_{30} = 2.1 \times 10^9$	34–36
Reactions of sulfate ions[c]			
31	$SO_4^{2-} + Cl^{\bullet} \rightleftarrows SO_4^{\bullet -} + Cl^-$	$k_{31} = 2.5 \times 10^8$, $k_{-31} = 6.1 \times 10^8$	37

[a] Fe(III) represents the Fe(III) species (Fe^{3+}, $FeCl^{2+}$ and $FeCl_2^+$). [b] Unless otherwise indicated, the rate constant values were the ones that best fit our experimental data. [c] Due to the sulfate impurity present in the inorganic salts used for adjusting the ionic strength or the pH.

incident irradiation. Photolysis of $Fe(Cl)^{2+}$ produces Fe^{2+} and chlorine atoms[26] with a $\phi_{347\ nm}$ of 0.47.[10] (eqn (6)).

Table 2 lists the additional reactions that must be considered in modelling the photolysis of Fe(III) species in the presence of chloride ions. In addition to the speciation to form $FeCl^{2+}$ and $FeCl_2^+$ (reactions 19–20, Table 2), there are reactions with chlorine species (21 and 22, Table 2), and reactions of chlorine-containing species (reactions 23–30, Table 2) that consume ferrous ions. The formation of sulfate anion radicals from the reaction of sulfate ions with chlorine atoms (reaction 31, Table 2) has been taken into account, since inorganic salts (sodium perchlorate, and sodium chloride) employed in this work could have sulfate ions as impurities. Fig. 1B and 1D show that the kinetic model fits the experimental data quite well.

The presence of sulfate ions in the aqueous solution can also affect the amounts of free ferrous and ferric ions. Sulfate ions complex with ferrous and ferric ions, forming $FeSO_4$, $FeSO_4^+$ and $Fe(SO_4)_2^-$ with equilibrium constants of 22.9 mol^{-1} L, 389 mol^{-1} L and 4470 mol^{-2} L^2, respectively, at an ionic strength of 0.1.[18] These equilibrium constants vary with ionic strength, as demonstrated in the literature.[27] At an ionic strength of 1.0, equilibrium constants of 120 mol^{-1} L and 900 mol^{-2} L^2 have also reported for $FeSO_4^+$ and $Fe(SO_4)_2^-$, respectively.[28]

At pH 3.0, $Fe(OH)^{2+}$ and $FeSO_4^+$ are the major ionic ferric species.[22] The molar absorptivity[21] of $FeSO_4^+$ is $\varepsilon_{350} = 576$ mol^{-1} L cm^{-1} and irradiation of $FeSO_4^+$ produces ferrous and sulfate radical anions with a very low quantum yield of 0.0016 at 350 nm.[21] (eqn (7)).

Table 3 shows all of the additional reactions that can occur in the photolysis of Fe(III) in the presence of sulfate anions (Fig. 1C). Under acidic conditions, HSO_4^- (reaction 35, Table 3) can competitively scavenge the hydroxyl radical (reaction 36, Table 3), producing the sulfate anion radical with a rate constant of 3.5×10^5 mol^{-1} L s^{-1}.[27] This latter species affects the reactivity of the reactive oxygen species (reactions 37 to 41, Table 3), and the consumption of ferrous ions (reaction 42, Table 3).

3.1. Kinetic modelling of the net Fe^{2+} production

The modelling of the formation of Fe^{2+} under continuous irradiation was carried out using the ground state reactions and rate constants listed in Tables 1 to 3, together with suitable mass balance relationships. The initial concentrations of $Fe(OH)^{2+}$, $Fe(OH)_2^+$, $FeCl^{2+}$ and $FeCl_2^+$, as well as the ferric and chloride ion concentrations, were calculated at pH 3.0 or 1.0 at the experimental ionic strength of 1.0 with the aid of the public domain speciation program Hydra (http://web.telia.com/~15651596/), employing the equilibrium constants for complexation supplied with the program. The molar absorptivities[21,23,25] were taken from the literature. The molar absorptivities of the species at 356 nm were taken into account, because the UV lamp employed in this work has maximum intensity at this wavelength.

Table 3 Additional reactions employed in the kinetic model for the photolysis of Fe(III) ions in aqueous solution in the presence of sulfate ions ($I = 1$)

No.	Reaction	k/s^{-1} or mol^{-1} L s^{-1}	Ref.
Speciation equilibria ($I = 1$)			
32	$Fe^{3+} + SO_4^{2-} \rightleftarrows FeSO_4^+$	$k_{32} = 2.09 \times 10^{12}$[a], $k_{-32} = 1 \times 10^{10}$ $k_{32} = 2.32 \times 10^{12}$ ($I = 1$)	27
33	$Fe^{3+} + 2SO_4^{2-} \rightleftarrows Fe(SO_4)_2^-$	$k_{33} = 1.95 \times 10^{13}$[a], $k_{-33} = 1 \times 10^{10}$ $k_{33} = 3.29 \times 10^{13}$ ($I = 1$)	27
34	$Fe^{2+} + SO_4^{2-} \rightleftarrows FeSO_4$	$k_{34} = 1.55 \times 10^{11}$[a], $k_{-34} = 1 \times 10^{10}$ $k_{34} = 1.19 \times 10^{11}$ ($I = 1$)	27
Reactions of sulfate ions			
35	$H^+ + SO_4^{2-} \rightleftarrows HSO_4^-$	$k_{35} = 2.8 \times 10^{11}$[a], $k_{-35} = 1 \times 10^{10}$ $k_{35} = 1.45 \times 10^{11}$ ($I = 1$)	27
36	$HSO_4^- + HO^\bullet \rightarrow SO_4^{\bullet-} + H_2O$	$k_{36} = 3.5 \times 10^5$	27
37	$SO_4^{\bullet-} + H_2O \rightarrow H^+ + SO_4^{2-} + HO^\bullet$	$k_{37} = 6.6 \times 10^2$	27
38	$SO_4^{\bullet-} + OH^- \rightarrow SO_4^{2-} + HO^\bullet$	$k_{38} = 1.4 \times 10^7$	27
39	$SO_4^{\bullet-} + H_2O_2 \rightarrow SO_4^{2-} + H^+ + HO_2^\bullet$	$k_{39} = 1.2 \times 10^7$	27
40	$SO_4^{\bullet-} + HO_2^\bullet \rightarrow SO_4^{2-} + H^+ + O_2$	$k_{40} = 3.5 \times 10^9$	27
41	$SO_4^{\bullet-} + SO_4^{\bullet-} \rightarrow S_2O_8^{2-}$	$k_{41} = 2.7 \times 10^8$	27
Reactions of iron species			
42	$Fe^{2+} + SO_4^{\bullet-} \rightarrow Fe^{3+} + SO_4^{2-}$	$k_{42} = 3.0 \times 10^8$	27

[a] Unless otherwise indicated, the rate constant values were the ones that best fit our experimental data.

The rate constants of the ionic species listed in Tables 1 to 3 refer to the ionic strength of 1.0. Thus, for example, considering all the above assumptions, the reactions of the hydroxyl radical and chlorine atoms can be described as:

$$\frac{d[HO^\bullet]}{dt} = I_0 f_{abs} \left\{ \frac{\left([FeOH^{2+}]\varepsilon_{FeOH^{2+}} + [Fe(OH)_2^+]\varepsilon_{Fe(OH)_2^+} \right)\Phi}{A} \right\} \frac{1}{V} \tag{43}$$

$$\begin{aligned} &-k_{11}[HO^\bullet]^2 - k_{12}[HO^\bullet][H_2O_2] + k_{14}[H_2O_2][HO_2^\bullet] - k_{15}[Fe^{2+}][HO^\bullet] \\ &+ k_{16}[Fe^{2+}][H_2O_2] - k_{28}[Cl^-][HO^\bullet] + k_{-28}[HOCl^{\bullet-}] \\ &- k_{36}[HSO_4^-][HO^\bullet] + k_{37}[SO_4^{\bullet-}] + k_{38}[SO_4^{\bullet-}][OH^-] \end{aligned}$$

$$\begin{aligned} \frac{d[Cl^\bullet]}{dt} &= I_0 f_{abs} \\ &\times \left\{ \frac{\left([FeOH^{2+}]\varepsilon_{FeOH^{2+}} + [Fe(OH)_2^+]\varepsilon_{Fe(OH)_2^+} \right)\Phi + \left([FeCl^{2+}]\varepsilon_{FeCl^{2+}} + [FeCl_2^+]\varepsilon_{FeCl_2^+} \right)\Phi}{A} \right\} \frac{1}{V} \end{aligned} \tag{44}$$

$$\begin{aligned} &-k_{21}[Fe^{2+}][Cl^\bullet] - k_{23}[Cl^\bullet][Cl^-] + k_{-23}[Cl_2^{\bullet-}] - k_{24}[Cl^\bullet][H_2O_2] \\ &+ k_{29}[HOCl^{\bullet-}][H^+] - k_{-29}[Cl^\bullet] - k_{30}[Cl_2^{\bullet-}][Cl^\bullet] - k_{31}[SO_4^{2-}][Cl^\bullet] \\ &+ k_{-31}[SO_4^{\bullet-}][Cl^-] \end{aligned}$$

where

$$\begin{aligned} A = &[FeOH^{2+}]\varepsilon_{FeOH^{2+}} + [Fe(OH)^+{}_2]\varepsilon_{Fe(OH)^+{}_2} \\ &+ [[Fe_2(OH)_2]^{4+}]\varepsilon_{[Fe_2(OH)_2]^{4+}} + [FeCl^{2+}]\varepsilon_{FeCl^{2+}} + [FeCl_2{}^+]\varepsilon_{FeCl_2{}^+} \\ &+ [FeSO_4]\varepsilon_{FeSO_4} + [FeSO_4{}^+]\varepsilon_{FeSO_4{}^+} \end{aligned} \tag{45}$$

These equations take into account the fraction of the incident light that is absorbed times the ratio between all complexes responsible for the hydroxyl or chlorine radicals production and all the species capable of the absorption of the irradiation light present in a fixed volume of the solution under studied.

Two sets of ordinary differential equations that describe the initial irradiation of the system were solved by optimizing the rates of the two primary processes for photochemical production of Fe^{2+} from either $Fe(OH)^{2+}$ or $FeCl^{2+}$ (reactions 8,9—Table 1 and reactions 19,20—Table 2, respectively).

For this purpose, a computational algorithm based on multivariable parametric optimization was applied, using MATLAB 6.5.[29] This algorithm involves the following steps: (i) an initial estimate of the parameters; (ii) the simultaneous solution of the system of differential equations by a standard fourth-order Runge–Kutta algorithm; (iii) the calculation of the objective function (OF) value, defined as:

$$OF = \sum_{t=1}^{n} ([Fe^{2+}]_{i\,exp.} - [Fe^{2+}]_{i\,calcd})^2 \tag{46}$$

where $[Fe^{2+}]_i$ is the ferrous ion concentration at the reaction time "i" and the indices "exp." and "calcd" refer to the experimental and calculated values and (iv) verification whether the objective function was within the stipulated tolerance. If not, new values for the rates of the two primary photochemical processes were estimated using a multivariate optimization method (Simplex method)[30] until the required tolerance was achieved.

Not surprisingly, the mechanistic steps with the fastest rate constants ($\geq 10^7$ mol^{-1} L s^{-1} or s^{-1}) are the ones that influence the net yield of Fe^{2+} the most. In the absence of both sulfate and chloride ions, both hydroxyl radical and hydrogen peroxide derived from hydroxyl radical are responsible for the consumption of Fe(II) (reactions 17, 18—Table 1). At long irradiation times (longer than 1000 s, Fig. 1A), a steady-state plateau is reached due to the simultaneous formation and consumption of Fe(II).

The presence of chloride ions in the solution results in formation of $FeCl^{2+}$ with a higher quantum yield of production of Fe(II).[16,26] There is a significant difference in the rate of formation of Fe^{2+} in the presence of chloride ions at pH 3.0 and 1.0 (Fig. 2). At both pHs, there is a rapid formation of chlorine atoms (eqn (6)). According to our kinetic model, the ratios of chlorine atoms and hydroxyl radicals ($Cl^{\bullet}/HO^{\bullet}$) produced under these conditions are 100 and 1×10^4 at pH 3.0 and 1.0, respectively. At pH 1.0, however, hydroxyl radical is quickly scavenged *via* pH dependent reactions with chlorine species (reactions 28, 29—Table 2) to form chlorine atoms. Reactions 23 to 30 of Table 2 are the preferential path for chlorine species to react, which lead the higher formation of Fe(II) as compared to pH 3.0 (Fig. 2).

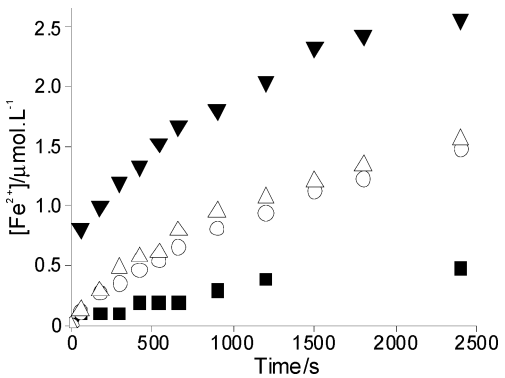

Fig. 2 Experimental data for the formation of ferrous ion during continuous irradiation experiments at pH 1.0 (▼) $[Cl^-] = 0.75$ mol L^{-1}, and absence of sulfate ions; pH 3.0: (○) in the absence of sulfate and chloride ions; (△) $[Cl^-] = 0.75$ mol L^{-1}, and absence of sulfate ions; and (■) $[SO_4^{2-}] = 1.8$ mmol L^{-1} and absence of chloride ions.

In the presence of sulfate ions, the ratio of hydroxyl radical to sulfate anion radical ($HO^{\bullet}/SO_4^{\bullet-}$) calculated from our kinetic model is 35. However, the overall effect of the presence of sulfate ions at longer irradiation time (Fig. 2) is to quench the formation of ferrous ions more efficiently than in the presence of chloride ions.

4. Conclusion

A kinetic model based on the principal reactions that occur in the system fits the data for formation of Fe^{2+} satisfactorily. Both experimental data and model prediction show that the availability of Fe^{2+} produced by photolysis of Fe^{3+} decreases much more in the presence of sulfate ion than in presence of chloride ion as a function of the irradiation time.

At pH 3.0, the photochemical step of the photo-Fenton reaction can be strongly inhibited by relatively low concentrations of sulfate ions, which complex with both ferrous and ferric ions, forming, respectively, $FeSO_4$, and $FeSO_4^+$. Sulfate ions are also capable of competitively scavenging $HO^{\bullet}$, thus further affecting the overall reactivity. Two common sources of sulfate ions in photo-Fenton systems are the use of a ferric or ferrous sulfate salt as the source of the iron added to the system or of H_2SO_4 to adjust the solution pH.

Acknowledgements

The authors thank the Centro de Capacitação e Pesquisa em Meio Ambiente (http://www.cepema.usp.br/) for providing facilities, CNPq and CAPES (project CAPES-CEPEMA) for financial and fellowship support.

References

1 O. Legrini, E. Oliveros and A. M. Braun, Photochemical processes for water treatment, *Chem. Rev.*, 1993, **93**, 671–698.
2 C. A. O. Nascimento, A. C. S. C. Teixeira, R. Guardani, F. H. Quina and J. Lopez-Gejo, Degradación fotoquímica de compuestos orgánicos de origen industrial, in *Quimica Sustentable en Lationoamerica*, ed. N. Nudelman, *Editora de la Universidad Nacional del Litoral*, Santa Fe, Argentina, 2004, pp. 205–220.
3 M. T. Emett and G. H. Khoe, Photochemical oxidation of arsenic by oxygen and iron in acidic solutions, *Water Res.*, 2001, **35**, 649–656.
4 S. L. Orozco, E. R. Bandala, C. A. Arancibia-Bulnes, B. Serrano, R. Suárez-Parra and I. Hernández-Pérez, Effect of iron salt on the color removal of water containing the azo-dye reactive blue 69 using photo-assisted Fe(II)/H_2O_2 and Fe(III)/H_2O_2 systems, *J. Photochem. Photobiol., A*, 2008, **198**, 144–149.
5 H. Katsumata, K. Matsuba, S. Kaneco, T. Suzuki, K. Ohta and Y. Yobiko, Degradation of carbofuran in aqueous solution by Fe(III) aqua complexes as effective photocatalysts, *J. Photochem. Photobiol., A*, 2005, **170**, 239–245.
6 A. Machulek Jr., E. Gogritchiani, J. E. F. Moraes, F. H. Quina, A. M. Braun and E. Oliveros Kinetic, mechanistic investigation of the ozonolysis of 2,4-xylidine (2,4-dimethyl-aniline) in acidic aqueous solution, *Sep. Purif. Technol.*, 2009, **67**, 141–148.
7 M. Zahorodna, E. Oliveros, M. Wörner, R. Bogoczek and A. M. Braun, Dissolution and mineralization of ion exchange resins: differentiation between heterogeneous and homogeneous (photo-)Fenton processes, *Photochem. Photobiol. Sci.*, 2008, **7**, 1480–1492.
8 J. J. Pignatello, E. Oliveros and A. MacKay, Advanced oxidation processes for organic contaminant destruction based on the Fenton reaction and related chemistry, *Crit. Rev. Environ. Sci. Technol.*, 2006, **36**, 1–84.
9 L. Lopes, J. De Laat and B. Legube, Charge transfer of iron(III) monomeric and oligomeric aqua hydroxo complexes: semiempirical investigation into photoactivity, *Inorg. Chem.*, 2002, **41**, 2505–2517.
10 J. Kiwi, A. Lopez and V. Nadtochenko, Mechanism and kinetics of the OH-radical intervention during Fenton oxidation in the presence of a significant amount of radical scavenger (Cl^-), *Environ. Sci. Technol.*, 2000, **34**, 2162–2168.
11 S. H. Bossmann, E. Oliveros, S. Göb, S. Siegwart, E. P. Dahlen, L. Payawan Jr., M. Straub, M. Wörner and A. M. Braun, New evidence against hydroxyl radicals as reactive intermediates in the thermal and photochemically enhanced Fenton reactions, *J. Phys. Chem. A*, 1998, **102**, 5542–5550.
12 S. H. Bossmann, E. Oliveros, M. Kantor, S. Niebler, A. Bonfill, N. Shahin, M. Worner and A. M. Braun, New insights into the mechanisms of the thermal Fenton reactions occurring using different iron(II) complexes, *Water Sci. Technol.*, 2004, **49**, 75–80.
13 S. V. Kryatov, E. V. Rybak-Akimova and S. Schindler, Kinetics and mechanisms of formation and reactivity of non-heme iron oxygen intermediates, *Chem. Rev.*, 2005, **105**, 2175–2226.
14 J. E. F. Moraes, F. H. Quina, C. A. O. Nascimento, D. N. Silva and O. Chiavone-Filho, Treatment of saline wastewater contaminated with hydrocarbons by the photo-Fenton process, *Environ. Sci. Technol.*, 2004, **38**, 1183–1187.
15 R. Maciel, G. L. Sant'Anna Jr. and M. Dezotti, Phenol removal from high salinity effluents using Fenton's reagent and photo-Fenton reactions, *Chemosphere*, 2004, **57**, 711–719.
16 A. Machulek Jr., C. Vautier-Giongo, J. E. F. Moraes, C. A. O. Nascimento and F. H. Quina, Laser flash photolysis study of the photocatalytic step of the photo-Fenton reaction in saline solution, *Photochem. Photobiol.*, 2006, **82**, 208–212.
17 A. Machulek Jr., J. E. F. Moraes, C. Vautier-Giongo, C. A. Silverio, L. C. Friedrich, C. A. O. Nascimento, M. C. Gonzalez and F. H. Quina, Abatement of the inhibitory effect of chloride anions on the photo-Fenton process, *Environ. Sci. Technol.*, 2007, **41**, 8459–8463.

18 J. De Laat, G. Truong Le and B. Legube, A comparative study of the effects of chloride, sulfate and nitrate ions on the rates of decomposition of H_2O_2 and organic compounds by Fe(II)/H_2O_2 and Fe(III)/H_2O_2, *Chemosphere*, 2004, **55**, 715–723.
19 J. C. Scaiano, *CRC handbook of organic photochemistry*, CRC Press Inc., Boca Raton, 1989.
20 J. G. Calvert and J. N. Pitts, Jr., *Photochemistry*, Wiley, New York, 1966.
21 H.-J. Benkelberg and P. Warneck, Photodecomposition of iron(III) hydroxo and sulfato complexes in aqueous solution: wavelength dependence of OH and SO_4^- quantum yields, *J. Phys. Chem.*, 1995, **99**, 5214–5221.
22 W. Feng and D. Nasheng, Photochemistry of hydrolytic iron(III) species and photoinduced degradation of organic compounds. A mini review, *Chemosphere*, 2000, **41**, 1137–1147.
23 R. H. Byrne and D. R. Kester, Ultraviolet spectroscopic study of ferric hydroxide complexation, *J. Solution Chem.*, 1978, **7**, 373–383.
24 C. H. Langford and J. H. Carey, The charge transfer photochemistry of the hexaaquoiron(III) ion, the chloropentaaquoiron(III) ion, and the μ-dihydroxo dimer explored with *tert*-butyl alcohol scavenging, *Can. J. Chem.*, 1975, **53**, 2430–2435.
25 R. H. Byrne and D. R. Kester, Ultraviolet spectroscopic study of ferric equilibria at high chloride concentrations, *J. Solution Chem.*, 1981, **10**, 51–67.
26 V. Nadtochenko and J. Kiwi, Photolysis of $FeOH^{2+}$ and $FeCl^{2+}$ in aqueous solution. Photodissociation kinetics and quantum yields, *Inorg. Chem.*, 1998, **37**, 5233–5238.
27 J. De Laat and G. Truong Le, Kinetics and modelling of the Fe(III)/H_2O_2 system in the presence of sulfate in acidic aqueous solutions, *Environ. Sci. Technol.*, 2005, **39**, 1811–1818.
28 G. G. Jayson, B. J. Parsons and A. J. Swallow, Appearance of sulfatoferric complexes in the oxidation of ferrous sulfate solutions. A study by pulse radiolysis, *J. Chem. Soc., Faraday Trans. 1*, 1973, **69**, 1079–1089.
29 *MATLAB® Optimization Toolbox©*, The MathWorks Inc., Natick, MA, USA, 1994–2005, www.mathworks.com..
30 W. H. Press, B. P. Flannery, S. A. Teukolsky and W. T. Vetterling, *Numerical recipes in Fortran 77: the art of scientific computing*, Cambridge University Press, Cambridge, 2nd edn, 1992.
31 J. De Laat and T. G. Le, Effects of chloride ions on the iron(III)-catalyzed decomposition of hydrogen peroxide and on the efficiency of the Fenton-like oxidation process, *Appl. Catal., B*, 2006, **66**, 137–146.
32 N. Kang, D. S. Lee and J. Yoon, Kinetic modelling of Fenton oxidation of phenol and monochlorophenols, *Chemosphere*, 2002, **47**, 915–924.
33 J. M. Joseph, R. Varghese and C. T. Aravindakumar, Photoproduction of hydroxyl radicals from Fe(III)-hydroxy complex: a quantitative assessment, *J. Photochem. Photobiol., A*, 2001, **146**, 67–73.
34 X.-Y. Yu and J. R. Barker, Hydrogen peroxide photolysis in acidic aqueous solutions containing chloride ions I. Chemical mechanism, *J. Phys. Chem. A*, 2003, **107**, 1313–1324.
35 X.-Y. Yu and J. R. Barker, Hydrogen peroxide photolysis in acidic aqueous solutions containing chloride ions II. Quantum yield of $HO^{\bullet}$ (aq) radicals, *J. Phys. Chem. A*, 2003, **107**, 1325–1332.
36 X.-Y. Yu, Critical evolution of rate constants and equilibrium constants of hydrogen peroxide photolysis in acidic aqueous solutions containing chloride ions, *J. Phys. Chem. Ref. Data*, 2004, **33**, 747–763.
37 G. V. Buxton, M. Bydder and G. A. Salmon, The reactivity of chlorine atoms in aqueous solution part II. The equilibrium $SO_4^{\bullet-} + Cl^- \rightleftharpoons Cl^{\bullet} + SO_4^{2-}$, *Phys. Chem. Chem. Phys.*, 1999, **1**, 269–273.